Counterion Distribution Enclosed in a Cylinder and a Sphere

Heng-Kwong Tsao

Department of Chemical Engineering, National Central University, Chung-li, Taiwan 32054, Republic of China

Received: June 18, 1998

The electric potential and counterion distributions within a cylinder and a sphere have been obtained analytically by solving the Poisson−Boltzmann equation exactly. The existence of the upper limit of the counterion concentration at the center of the aqueous core has been observed regardless of the surface charge density. This result indicates that, at very high surface charge density, most of the counterions are strongly attracted to the surroundings of the surface and to balance the charges on the surface.

1. Introduction

Water-in-oil microemulsions (W/O) and swollen reverse micelles have been investigated extensively over the past decade or so. These microdroplets can be used as microreactors for manufacturing both organic[1] and inorganic[2−4] nanosized particles. In addition, the solubilization of macromolecules, such as enzymes, in the oil phase could provide many opportunities for the development of new biocatalytic reactions in the organic solvents.[5,6] In understanding the structure and thermodynamics of W/O microemulsions,[7−9] the electrical contribution associated with the electric double layer in the aqueous core due to the dissociation of the ionic surfactants plays an important role, besides the bending free energy associated with the hydrophobic tail of the surfactants. In addition, the electric conductivity of W/O microemulsions, which may be explained by the charge fluctuation model,[10] is also significantly affected by the counterion distribution in the aqueous core.

The diffuse electric double layer is often described by the Poisson−Boltzmann (PB) equation. Though more rigorous methods such as molecular simulations and more sophisticated approaches such as numerical solution of the integral equations (e.g., PY and HNC) can be applied to higher ion concentrations,[11] the PB equation is relatively simple, and the results are often accurate. The diffuse double layers near a flat plate, outside a cylinder, and around a spherical particle have been extensively studied.[12] Recently, considerable theoretical interest has been attracted to the ion distribution inside a cylinder and a sphere because of the numerous studies on the systems of microemulsions, reverse micelles, and vesicles.[7,8,13−16] Though the electric potential inside a cylinder and a sphere can be solved for a linearized PB equation,[16] in general, it is believed that for high potential and spherical symmetry no close solution exists for the PB equation.[7,14,15] Approximate solutions in cylindrical and spherical diffuse layers can be obtained for thin double layers, i.e., $\kappa a \gg 1$. Here κ and a are the inverse Debye length and the radius of the particle, respectively. On the basis of a series expansion in $1/\kappa a$ for the electric potential up to terms of order $1/(\kappa a)^2$, analytical expressions by Lekkerkerker et al.[14,15] for the surface potential are found to be accurate within 2% when $\kappa a \geq 2$.

Most of the previous studies[7−9,14−16] neglect the counterions dissociated from the ionic surfactants due to high concentrations of the added electrolyte. For a W/O microemulsion system and reverse micelles, in general, the total charge of the droplet is not zero, but the magnitude of the net charge is much less than the total charge on the surface.[10,17] The whole system (both the aqueous core and the ionic surfactant shell) is thus assumed to satisfy the condition of electroneutrality. As a result, the net charge in the aqueous core is approximately equal to the total counterions dissociated from the ionic surfactant shell whether the salt is added or not. Usually, the contribution from counterions cannot be neglected in a W/O droplet microemulsion unless a large amount of inorganic salt is added. For instance, there is $O(100-10000)$ counterions dissociated from the surfactant shell for a droplet of radius 10 nm, but about 25 Na^+ (Cl^-) ions exist for 0.01 M NaCl.

In this paper, on the basis of the PB equation, we study the electrostatic field enclosed in a charged surface with counterions only. We consider three cases including one, two, and three dimensions. Here the solutions between two planar plates can be considered as an enclosed system in one dimension instead of a simple model of two-particle interactions.[17,18] The solutions within an infinite cylinder and a sphere can be regarded as two- and three-dimensional problems, respectively. The electric potential and the distribution of counterions are first solved in terms of the series solutions. Then the concise, analytical forms of the electrical potential can be obtained for both rectangular and cylindrical coordinates. An accurate approximate solution for the spherical coordinate can also be obtained analytically by the Padé approximant.

2. Exact Solution

Consider an aqueous core enclosed by an ionic surfactant shell depicted in Figure 1. The only ions in the water pool are those that come off the inner surfaces. We consider three cases, including two similarly charged planar surfaces, a hollow cylinder, and a spherical cavity. The electric potential ϕ^* in the solution can be described by the Poisson−Boltzmann equation

$$\frac{1}{r^m}\frac{\mathrm{d}}{\mathrm{d}r}\left(r^m\frac{\mathrm{d}\phi^*}{\mathrm{d}r}\right) = -\frac{n_c^0 z_c e}{\epsilon_r \epsilon_0}\exp\left(\frac{-z_c e\phi^*}{kT}\right) \qquad (1)$$

where n_c^0 and z_c are the number density at $r = 0$ and valency, respectively, of the counterions dissociated from the surfactant shell. ϵ_r is the dielectric constant of the solution, and ϵ_0 is the permittivity of a vacuum. e stands for the fundamental charge, 1.6×10^{-19}C. Note that $m = 0$ for rectangular coordinates, $m = 1$ for cylindrical coordinates, and $m = 2$ for spherical coordinates.

10.1021/jp982689o CCC: $15.00
Published on Web 11/13/1998

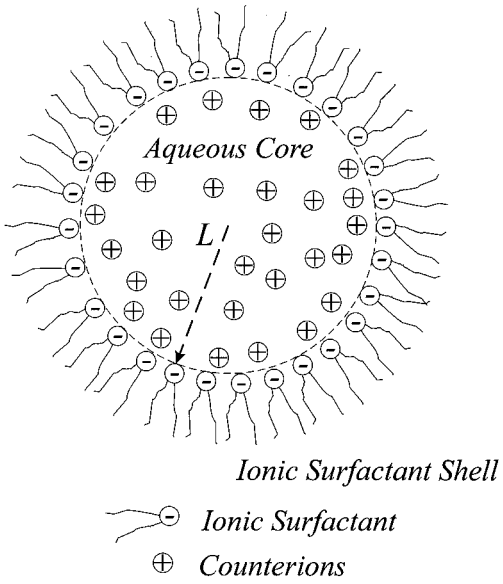

Figure 1. Counterions in the aqueous core enclosed in an ionic surfactant shell. The system size is 2*L*.

Let 2*L* denotes the characteristic size of the system, for example, the separation distance between two surfaces, the diameter of the cylinder or sphere. If one defines

$$x = \frac{r}{L} \quad \text{and} \quad \phi = \frac{\phi^*}{kT/z_c e} \tag{2}$$

then the PB equation becomes

$$\frac{1}{x^m}\frac{\mathrm{d}}{\mathrm{d}x}\left(x^m \frac{\mathrm{d}\phi}{\mathrm{d}x}\right) = -(\kappa_c L)^2 \exp(-\phi) \tag{3}$$

where

$$\kappa_c^2 = \frac{n_c^0 z_c^2 e^2}{\epsilon_r \epsilon_0 kT} \tag{4}$$

Equation 3 is a nonlinear ordinary differential equation, which is subject to the symmetry condition

$$\frac{\mathrm{d}\phi}{\mathrm{d}x} = 0, \quad \text{at} \quad x = 0 \tag{5}$$

and the condition of constant surface charge density σ

$$\frac{\mathrm{d}\phi}{\mathrm{d}x} = \Lambda, \quad \text{at} \quad x = 1 \tag{6}$$

where $\Lambda = L\sigma z_c e/\epsilon_r \epsilon_0 kT \leq 0$ since σ and z_c are in opposite sign.

Assume the solution of eq 3 can be expressed as an infinite series

$$\phi(x) = \sum_{n=0}^{\infty} a_n x^n \tag{7}$$

where a_0 corresponds to the potential at $x = 0$. With the boundary condition (eq 5), one has

$$a_1 = 0$$

Substituting eq 7 into the PB equation and expanding the exponential term on the right-hand side of eq 3 in Taylor series gives

$$\sum_{n=1}^{\infty} n(n+m-1)a_n x^{n-2} = -(\kappa_c L)^2 \sum_{n=0}^{\infty} (-1)^n \frac{\phi^n}{n!} \tag{8}$$

Since the various powers of x in eq 7 are linearly independent, the equality can be established if and only if the coefficient of each power of x is equal at both sides. Thus we obtain the linear recurrence relations

x^{-1}: $ma_1 = 0$

x^0: $2(m+1)a_2 = -(\kappa_c L)^2 \exp(-a_0)$

x^1: $3(m+2)a_3 = (\kappa_c L)^2 a_1 \exp(-a_0)$

x^2: $4(m+3)a_4 = (\kappa_c L)^2 a_2 \exp(-a_0)$

x^4: $6(m+5)a_6 = -(\kappa_c L)^2\left(-a_4 + \frac{a_2^2}{2}\right)\exp(-a_0)$

x^6: $8(m+7)a_8 = -(\kappa_c L)^2\left(-a_6 + a_4 a_2 - \frac{a_2^3}{6}\right)\exp(-a_0)$

x^8: $10(m+9)a_{10} =$
$$-(\kappa_c L)^2\left(-a_8 + a_6 a_2 + \frac{a_4^2}{2} - \frac{a_4 a_2^2}{2} + \frac{a_2^4}{4!}\right)\exp(-a_0)$$

In general, $a_{2k+2}/[(\kappa_c L)^2 \exp(-a_0)]$ can be expressed in terms of a_{2i} with $i \geq 1$.

x^{2k+2}: $(2k+2)(m+2k+1)a_{2k+2} =$
$$-(\kappa_c L)^2\left\{-a_{2k} + \left[\sum_{i\neq k} a_i a_{2k-i} + \frac{a_k^2}{2}\right] - \left[\sum_{\substack{i\neq j\neq l \\ i+j+l=2k}} a_i a_j a_l + \frac{1}{2}\sum_{\substack{i\neq j \\ 2i+j=2k}} a_i^2 a_j\right] + \ldots + (-1)^k \frac{a_k^2}{k!}\right\}\exp(-a_0)$$

Note that the odd terms are all zero because they are proportional to a_1. Since only differences in electric potential are physically meaningful, one may set $\phi(x=0) = a_0 = 0$. According to the previous results, one has

$$a_2 = -\frac{1}{2(m+1)}(\kappa_c L)^2 \tag{9}$$

$$a_4 = -\frac{1}{8(m+1)(m+3)}(\kappa_c L)^4 \tag{10}$$

$$a_6 = -\frac{m+2}{24(m+1)^2(m+3)(m+5)}(\kappa_c L)^6 \tag{11}$$

$$a_8 = -\frac{3m^2+16m+17}{192(m+1)^3(m+3)(m+5)(m+7)}(\kappa_c L)^8 \tag{12}$$

$$a_{10} = -\frac{1}{960}\frac{(m+4)(6m^3+55m^2+134m+93)}{(m+1)^4(m+3)^2(m+5)(m+7)(m+9)}(\kappa_c L)^{10} \tag{13}$$

To determine $(\kappa_c L)^2$ (or n_c^0), one can substitute the potential

into the boundary condition

$$\Lambda = \sum_{k=1}^{\infty}(2k)a_{2k} = -\frac{(\kappa_c L)^2}{m+1}\left\{1 + \frac{(\kappa_c L)^2}{2(m+3)} + \frac{(m+2)(\kappa_c L)^4}{4(m+1)(m+3)(m+5)} + O[(\kappa_c L)^6]\right\} \quad (14)$$

For two planar plates, eq 14 reduces to

$$\left(\frac{\kappa_c L}{\sqrt{2}}\right)\tan\left(\frac{\kappa_c L}{\sqrt{2}}\right) = -\frac{\Lambda}{2} \quad (15)$$

This result indicates that $(\kappa_c L)^2 < \pi^2/2$ for $m = 0$. The electric potential is given by[18,19]

$$\phi = \ln\cos^2\left(\frac{\kappa_c L}{\sqrt{2}}x\right) \quad (16)$$

For a cylinder, eq 14 becomes

$$\frac{(\kappa_c L)^2}{8 - (\kappa_c L)^2} = -\frac{\Lambda}{4} \quad (17)$$

This result indicates that $(\kappa_c L)^2 < 8$ for $m = 1$. The electric potential is given by

$$\phi = \ln\left[1 - \frac{(\kappa_c L)^2}{8}x^2\right]^2 = \ln\left[1 - \frac{\Lambda}{\Lambda - 4}x^2\right]^2 \quad (18)$$

Knowing the electric potential at the surface, the electrostatic free energy can be obtained by the charging process.

$$f^* = \int_0^{\sigma}\phi^*(r = L; \sigma')\,d\sigma' = \frac{L}{\epsilon_r\epsilon_0}\int_0^{\Lambda}\phi(x = 1; \Lambda')d\lambda'$$

Using eq 18, one has the free energy associated with a cylinder

$$f^* = 2\frac{a}{\epsilon_r\epsilon_0}\left\{4 + (4 - \Lambda)\left[\ln\left(1 - \frac{\Lambda}{4}\right) - 1\right]\right\}$$

With eqs 9−13 and eq 14, one can also determine the electric potential within a sphere, i.e., $m = 2$. Unfortunately, we are unable to convert the series solution into a concise form. Since the truncated power series of the electric potential is unsatisfactory for $(-\Lambda) \gg 1$, a more sophisticated technique, Padé approximants, is adopted to approximate the solution. According to the results of both $m = 0$ and 1, one can assume $\phi = \ln h(x)^2$ with $0 < h(x) \leq 1$. Note that $h = 1$ at $x = 0$ and $h \to \infty$ when $\kappa_c L \to (\kappa_c L)_c$. We use the first four coefficients to construct the (3, 3) Padé approximant for the electric potential:

$$\phi(x; \Lambda) \cong \ln\left(\frac{1 - \frac{251}{2088}(\kappa_c L)^2x^2 + \frac{4421}{1753920}(\kappa_c L)^4x^4}{1 - \frac{77}{2088}(\kappa_c L)^2x^2 + \frac{83}{584640}(\kappa_c L)^4x^4}\right)^2 \quad (19)$$

The relation between $-\Lambda$ and $\kappa_c L$ can then be obtained from the boundary condition (eq 6). Equation 19 shows that the surface potential $\phi^s = \phi(x = 1)$ diverges when $(\kappa_c L)_c^2 = 10.735$. One can also use the first five coefficients to construct a (3, 3) Padé approximant for the $(-\Lambda) - \kappa_c L$ relation (14):

$$\Lambda \cong -\frac{(\kappa_c L)^2}{3}\left[\frac{1 - \frac{23}{825}(\kappa_c L)^2 - \frac{118}{2338875}(\kappa_c L)^4}{1 - \frac{211}{1650}(\kappa_c L)^2 + \frac{859}{267300}(\kappa_c L)^4}\right] \quad (20)$$

Equation 20 indicates that $\Lambda \to \infty$ when $(\kappa_c L)_c^2 = 10.694$. Both of them agree well with the numerical result $(\kappa_c L)_c^2 \cong 10.717$.

3. Asymptotic Analysis

In this section we discuss the limiting cases: high charge density $-\Lambda \gg 1$ and low charge density $-\Lambda \lesssim 1$. We derive, particularly for $m = 2$, the exact expressions of the surface potential ϕ^s, which is useful in evaluating the electrostatic free energy.

3.1. $(-\Lambda) \gg 1$. In the limit of $-\Lambda \gg 1$, the charge density and the electric potential at the surface in general can be related to the $\kappa_c L$ as

$$-\Lambda = f(\kappa_c L)\left(1 - \frac{(\kappa_c L)}{(\kappa_c L)_c}\right)^{-1} \quad (21)$$

and

$$\phi^s = \ln\left\{g(\kappa_c L)\left(1 - \frac{(\kappa_c L)}{(\kappa_c L)_c}\right)\right\}^2 \quad (22)$$

respectively. Both the functions $f(z)$ and $g(z)$ have no singularity at $z = (\kappa_c L)_c$. Inserting eq 21 into eq 22 yields

$$\phi^s \cong \ln\left\{\frac{f[(\kappa_c L)_c]\, g[(\kappa_c L)_c]}{-\Lambda}\right\}^2 \quad (23)$$

In other words, ϕ^s can be expressed as

$$\phi^s = -\ln\Lambda^2 + C_m[(\kappa_c L)_c] \quad (24)$$

where C_m is a constant, which depends on the geometry. This result indicates that for $-\Lambda \gg 1$, the leading behavior of the cylinder and sphere is the same as that of two planar plates. However, the next order terms are different due to the curvature effects. For $m = 0$, $(\kappa_c L)^2 \approx (\pi^2/2)(1 + (4/\Lambda))$ and $C_0 = \ln \pi^2$. For $m = 1$, $(\kappa_c L)^2 \approx 8(1 + (4/\Lambda))$ and $C_1 = \ln 4^2$. For $m = 2$, using eqs 20 and 6, one has $(\kappa_c L)^2 \approx (\kappa_c L)_c^2(1 + (4.0/\Lambda))$ and $C_2 \approx \ln(4.57)^2$. According to the numerical calculation, $C_2 \approx \ln(4.55)^2$.

The counterion concentration at the surface n_c^s can then be estimated as

$$n_c^s = n_c^0 e^{-\phi^s} \cong e^{-C_m}(\kappa_c L)_c^2\frac{\sigma^2}{\epsilon_r\epsilon_0 kT} = \alpha\frac{\sigma^2}{\epsilon_r\epsilon_0 kT} \quad (25)$$

We found that the constant $\alpha = {}^1/_2$ for the cases $m = 0$ and 1 and $\alpha \approx 0.51$ for $m = 2$. Since the former results are based on the exact solutions, one would suggest that α should also be ${}^1/_2$ for the spherical coordinate. That is, $C_m = \ln 2(\kappa_c L)_c^2$. This result shows that the concentration of counterions at the surface is proportional to the square of the charge density in the limit $-\Lambda \gg 1$.

3.2. $(-\Lambda) \lesssim O(1)$: Debye−Hückel Approximation. An approximate solution of the PB equation can be obtained under

the Debye−Hückel approximation. From eq 3, the exponential term in the PB equation can be linearized when $\phi \ll 1$.

$$\frac{1}{x^m}\frac{d}{dx}\left(x^m \frac{d\phi}{dx}\right) = -(\kappa_c L)^2(1-\phi)$$

By defining $\phi = 0$ at $x = 0$ and subject to the boundary conditions 5 and 6, the solutions are given as follow: For $m = 0$

$$\phi(x) = 1 - \cosh(\kappa_c L)x$$

with

$$(\kappa_c L)\sinh(\kappa_c L) = -\Lambda$$

For $m = 1$

$$\phi(x) = 1 - I_0(\kappa_c L)x$$

with

$$(\kappa_c L)I_1(\kappa_c L) = -\Lambda$$

where $I_n(x)$ is the modified Bessel functions of the first kind of order n. For $m = 2$, the electric potential is

$$\phi(x) = 1 - \frac{\sinh(\kappa_c L)x}{(\kappa_c L)x}$$

with $(\kappa_c L)$ determined by

$$\frac{(\kappa_c L)\cosh(\kappa_c L) - \sinh(\kappa_c L)}{(\kappa_c L)} = -\Lambda$$

Obviously, $(\kappa_c L)_c$ does not exist in this limit. One can also define $\phi = 0$ at the position where the concentration of the counterion, n_c, equals the average concentration $\bar{n}_c$. Owing to the electroneutrality condition, $(\bar{\kappa}_c L)^2 = -(m+1)\Lambda$. Here $\bar{\kappa}_c^2$ is defined based on $\bar{n}_c$. For $m = 2$, one has

$$\phi(x) = 1 - \left(\frac{\Lambda}{\sqrt{-3\Lambda}\cosh\sqrt{-3\Lambda} - \sinh\sqrt{-3\Lambda}}\right)\frac{\sinh(\sqrt{-3\Lambda}x)}{x}$$

4. Discussion and Conclusions

In this paper we investigate the counterion distribution within an enclosed charged surface. The system can be regarded as a solution within two charged plates for one-dimension, a cylinder for two-dimension, and a sphere for three-dimension. On the basis of the series expansion, the nonlinear Poisson−Boltzmann equation can be solved analytically. The profiles of the electric potential and the concentration of counterions are then obtained.

A typical microemulsion droplet of radius 10 nm contains $O(1000)$ ionic surfactants and an approximately equal amount of counterions in the aqueous core. If the surface charge density is as high as $\sigma = 0.2$ C/m^2 at 25 °C, $-\Lambda \approx 112$. Since $\Lambda \propto L$, larger droplets have higher values of $-\Lambda$. However, if only 20% dissociation of the counterions from the surfactant shell, then $-\Lambda \approx 22$. Addition of cosurfactant may reduce the surface charge density further. Therefore, an analytical expression of the electric potential, which is valid from low to high charge density, is useful in studying the microemulsion system.

Figure 2 illustrates the variation of the counterion concentration with the position within a cylinder for various surface charge densities. Note that $(\kappa_c L)_x^2$ denotes the concentration of counterion $n_c(x)$, which is nondimensionalized by $\epsilon_r\epsilon_0 kT/z_c^2 e^2 L^2$. As $-\Lambda \lesssim O(1)$, the concentration profile is close to uniform and the Debye−Hückel approximation is valid. When the charge density increases, one would expect that the concentration profile moves up because the average concentration is proportional to the charge density. As $-\Lambda \gtrsim O(100)$, the concentration increases very rapidly (several orders of magnitude) in the neighborhood of the charged shell since $n_c^s \propto \Lambda^2$ according to eq 25. However, the concentration profile is nearly uniform near the center and its value n_c^0 does not increase significantly with increasing $-\Lambda$. n_c^0 seems to reach an upper limit (~8). In other words, further increasing the surface charge density does not have any effect on the concentration of counterion at the center. Most of the counterions are strongly attracted to the surrounding of the surface and to balance the surface charge.

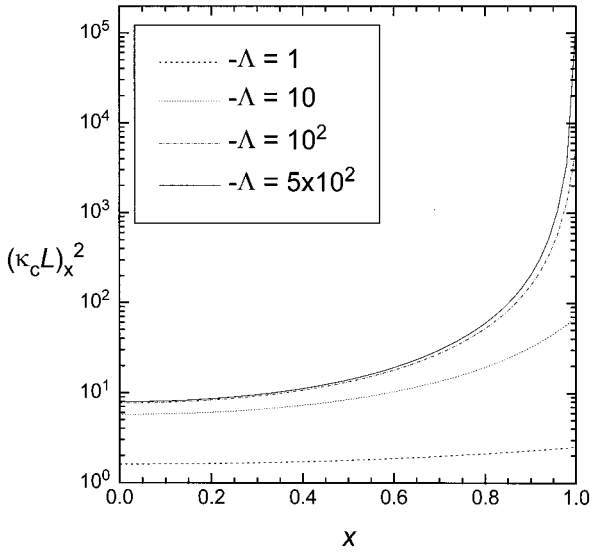

Figure 2. Variation of the dimensionless concentration of counterions $(\kappa_c L)_x^2$ with the dimensionless position x within a cylinder for various surface charge density.

It is known that for highly charged surfaces most of the counterions reside close to the surface owing to the Coulomb attractions.[17] However, one would also expect that the concentration of counterions at the center of the system would increase with increasing surface charge density owing to the entropy of mixing with the solvent. The existence of the upper limits of $\kappa_c L$ for different geometries is clearly shown in Figure 3, which demonstrates the relation between $(\kappa_c L)^2$ and $-\Lambda$. This result indicates that for a given L (e.g., the radius of a sphere), the concentration of counterions cannot exceed the value of $(\kappa_c L)_c^2$ regardless of the surface charge density or the total number of counterions within the system. On the other hand, when $-\Lambda \gtrsim O(100)$, the counterion concentration at the center varies only with L^{-2} despite the surface charge density. One can also see that the upper limits are in the order of $(\kappa_c L)_c^{m=2} > (\kappa_c L)_c^{m=1} > (\kappa_c L)_c^{m=0}$. This can be explained by the order of volume-to-surface ratio: $(L)_{m=0} > (L/2)_{m=1} > (L/3)_{m=2}$. Since the sphere has the lowest available volume for a given size L, it has the highest concentration of counterions at the center.

In the calculation of the electric potential for the system of a sphere, we have the exact solution in terms of power series, which gives correct values for $x(\kappa_c L)^2 \ll (\kappa_c L)_c^2$. To obtain the accurate result for $(-\Lambda) \gg 1$ or $(\kappa_c L)^2 \rightarrow (\kappa_c L)_c^2$, infinite terms have to be evaluated. As a consequence, we use the Padé

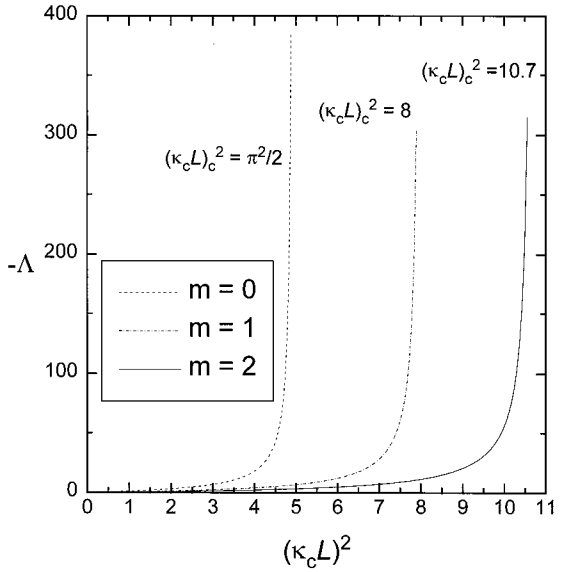

Figure 3. Variation of the surface charge density $-\Lambda$ with the dimensionless concentration of counterions at the center of the system $(\kappa_c L)^2$ for various geometry.

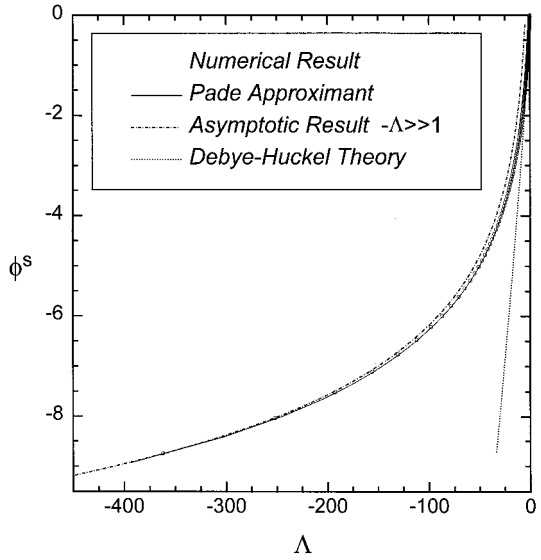

Figure 4. Surface potential ϕ^s for a sphere as a function of the surface charge density $-\Lambda$ for different approaches, including the numerical result, Padé approximant, asymptotic expression, and Debye−Hückel theory.

approximants to improve the convergence rate near the singularity. To test the accuracy of this approximation, we compare the result by the Padé approximant with that of the numerical calculation. Since the approximate solutions of the electric potential gives correct results for $x \ll 1$, the accuracy of them can be revealed by the electric potential at the surface ϕ^s. Figure 4 shows the variation of ϕ^s with the surface charge density $-\Lambda$. The result of Padé approximant agrees quite well with the numerical solution. This approximate solution shows correctly that ϕ^s diverges when $\kappa_c L = (\kappa_c L)_c$. It is believed that a (4, 4) Padé approximant can lead to an even higher accuracy by considering the first six coefficients in the series solution. The asymptotic expression (eq 24) for ϕ^s also gives a quite satisfactory result when $-\Lambda \gg 1$. Though the Debye−Hückel approximation is expected to be valid for $\phi \ll 1$, Figure 4 shows that it is good for $-\Lambda \lesssim 5$, which corresponds to $\phi^s \approx -2$.

It is worth noting that, for a given size L, if the surface charge density σ continues to increase, the assumption of point ions in the PB equation may break down, especially near the surface. The approaches that take into account the size of the ions, such as molecular simulations, are necessary to justify the accuracy of the PB equation. To apply our result to the microemulsion systems, further refinement such as the presence of a Stern layer and incomplete dissociation from the ionic surfactant shell have to be accounted for.

Acknowledgment. This research is supported by National Council of Science of Taiwan under Grant No. NSC 87-2214-E-008-009.

References and Notes

(1) Hammouda, A.; Gulik, Th.; Pileni, M. P. *Langmuir* **1995**, *11*, 3656.
(2) Stathatos, E.; Lianos, P.; Del Monte, F.; Levy, D.; Tsiourvas, D. *Langmuir* **1997**, *13*, 4295.
(3) Joselevich, E.; Willner, I. *J. Chem. Phys.* **1994**, *98*, 7628.
(4) Pileni, M. P. *J. Phys. Chem.* **1993**, *97*, 6961.
(5) Goklen, K. E.; Hatton, T. A. *Biotechnol. Prog.* **1985**, *1*, 69.
(6) Pitre, F.; Regnaut, C.; Pileni, M. P. *Langmuir* **1993**, *9*, 2855.
(7) Overbeek, J. Th., G.; Verhoeckx, G. J.; Bruyn, P. L. De; Lekkerkerker, H. N. W. *J. Colloid Interface Sci.* **1987**, *119*, 422.
(8) Rahaman, R. S.; Hatton, T. A. *J. Phys. Chem.* **1991**, *95*, 1799.
(9) Mitchell, D. J.; Ninham, B. W. *J. Phys. Chem.* **1983**, *87*, 2996.
(10) Bratko, D.; Woodward, C. E.; Luzar, A. *J Chem. Phys.* **1991**, *95*, 5318.
(11) McQuarrie, D. A. *Statistical Mechanics*; Harper & Row: New York; 1976; Chapter 15.
(12) Russel, W. B.; Saville, D. A.; Schowalter, W. R. *Colloidal Dispersion*; Cambridge University Press: Cambridge, 1989; Chapter 4.
(13) Bratko, D.; Luzar, A.; Chen, S. H. *J. Chem. Phys.* **1988**, *89*, 545.
(14) van Aken, G. A.; Lekkerkerker, H. N. W.; Overbeek, J. Th. G.; de Bruyn, P. L. *J. Phys. Chem.* **1990**, *94*, 8468.
(15) Lekkerkerker, H. N. W *Physica A* **1989**, *159*, 319.
(16) Winterhalter, M.; Helfrich, W. *J. Phys. Chem.* **1988**, *92*, 6865.
(17) Levine, S.; Robinson, K. *J. Phys. Chem.* **1972**, *76*, 876.
(18) Israelachvili, J. *Intermolecular Surface Forces*, 2nd ed.; Academic Press: San Diego, CA, 1992; Chapter 12.
(19) Safran, S. A. *Statistical Thermodynamics of Surfaces, Interfaces, and Membrane*; Addison-Wesley: Reading, MA, 1994; Chapter 5.